



## Supporting Online Material for

### **A Whiff of Oxygen Before the Great Oxidation Event?**

A. D. Anbar,\* Y. Duan, T. W. Lyons, G. L. Arnold, B. Kendall, R. A. Creaser, A. J. Kaufman, G. W. Gordon, C. Scott, J. Garvin, R. Buick

\*To whom correspondence should be addressed. E-mail: anbar@asu.edu

Published 28 September 2007, *Science* **317**, 1903 (2007)

DOI: 10.1126/science.1140325

**This PDF file includes:**

Materials and Methods  
Figs. S1 and S2  
Tables S1 to S3

**Supporting Online Materials**  
**for**  
***A Whiff of Oxygen before the Great Oxidation Event?***

***The Hamersley Core***

The Hamersley core was recovered during the summer of 2004 as part of the Deep Time Drilling Project (DTDP) of the Astrobiology Drilling Program (ADP) of the NASA Astrobiology Institute (NAI). This project also involved the Geological Survey of Western Australia, Randolph Resources, Hamersley Iron, SIPA Resources International, and the University of Western Australia. This was one of ten cores recovered by the ADP in 2003 – 2004; seven others were collected as part of the Archean Biosphere Drilling Project (ABDP) (I), and two others were collected in collaboration between the DTDP and the ABDP. Therefore, this core is sometimes referred to as “ABDP-9”. The motivation for recovery of this particular core was to obtain drill core free of modern contamination and weathering effects for biogeochemical analysis to characterize the nature of life and its environment in the late Archean, shortly before the rise of atmospheric oxygen.

Approximately 1000 m of continuous drill core spanning banded iron formation, kerogenous shales, basinal carbonates, shallower cherts and clastics, and meteorite impact horizons were recovered. The drill site was located at 21°59'29.5"S, 117°25'13.6"E, hole azimuth 186°, dip 89°, on the Pilbara craton of Western Australia (Figure S1). One half of the core is archived at the Geological Survey of Western Australia's (GSWA) Perth Core Library. The other (working) half of the core is presently stored at the School of Earth and Space Exploration at Arizona State University. For more information about the DTDP or how to request samples, please see <http://nai.nasa.gov/ADP/DTDP2004.cfm>.

***Lithostratigraphy and Sampling***

The core intersects laminated and well preserved sediments accumulated in a marine environment below wave base. These sediments have experienced only mild regional metamorphism (prehnite-pumpellyite facies to <300°C) and minimal deformation (gentle folding dips <5°). It is underlain by Mt. Sylvia Formation and capped by the Dales Gorge Member of the Brockman Iron Formation. The uppermost part is characterized by inter-bedded carbonates and grey/black shale with pyrite rarely to sparsely seen, gradually transiting into black shale with increasing pyrite content down section. Pyrite nodules occur massively from 131 m - 134 m followed by a 15 m thick section of black shale with frequent pyrite laminae and abundant pyrite nodules. Following this section, pyrite contents drops downcore as the lithology transitions to siderite banded iron formation (BIF). Continuing below 173 m depth, pyritic black shale becomes dominant again, with carbonate/marl interbeds, until the base of the Mt. McRae Shale. The core was sampled at 0.2 m ~ 2 m intervals for high-resolution analyses. For the purpose of this study sampling specifically avoided pyrite nodules. Laminae were avoided wherever possible. Where pyrite laminae were not avoidable (i.e., ~134 to 143 m) samples are labeled with a “pyl” suffix (Table S2).

### ***Metal Concentration Analyses***

Data are presented in Table S2. For each sample a billet was cut (3 cm x 5 cm x 1 cm) from the drill core using a water-cooled diamond blade tile saw. The billets were then broken into < 5 mm chips, without metal contact and ground to < 100 mesh in silicon nitride ball mill vials. For major and trace element analyses powder splits were completely dissolved using a standard HNO<sub>3</sub>-HCl-HF silicate digestion method. Trace HF was added to each solution to ensure Mo remained stable in solution. All dissolution and dilution was carried out in Class-10 workspaces within a trace metal cleanlab. Samples were analyzed on a Thermo Scientific X Series Q-ICP-MS (quadrupole inductively coupled plasma mass spectrometer) at the W.M. Keck Foundation Laboratory for Environmental Biogeochemistry at Arizona State University. Major elements (including Al, Fe, and Mn) and trace elements (including Mo, U and Re) were measured in separate analytical sessions against multiple element calibration standards. Internal standards Ge, In, Y and Bi, introduced into the instrument in parallel with all samples and standards, were used to correct for signal drift. Signal intensities for each analyte element were at least 3 times that of the blank and were bracketed by the lowest and the highest standard. Analyte concentration reproducibilities are better than 5 % except for low Re samples (when Re concentrations are ~1.5 ppb, the reproducibility drops to ~8 %). USGS geochemical reference materials SDO-1 and SCO-1, an organic rich and average shale, respectively, were measured alongside samples to assure measurement accuracy. Analyte concentrations produced for the reference materials agree within error of the published values.

### ***Re/Os Isochron***

Data are presented in Table S3. For Re/Os analysis, sample billets were cut at ASU as previously described and subsequently processed at the University of Alberta. Between 15 and 40 g of drillcore material was ground to remove cutting and drilling marks, broken into small chips without metal contact, and powdered in an automated agate mill. Re-Os isotope analyses were carried out at the Radiogenic Isotope Facility of the Department of Earth and Atmospheric Sciences, University of Alberta, using chemical separation and mass spectrometry methods outlined in Creaser et al. (2), Selby and Creaser (3) and Kendall *et al.* (4), including the Cr<sup>VI</sup>-H<sub>2</sub>SO<sub>4</sub> digestion protocol for organic-rich sedimentary rocks. This method minimizes release of detrital Re and Os from the silicate matrix in these rocks by selectively dissolving organic matter that is host to predominantly hydrogenous Re and Os (3, 4). Rhenium and Os are loaded onto Ni and Pt filaments, respectively, and analyzed by isotope dilution – negative thermal ionization mass spectrometry (ID-NTIMS). Regression of Re and Os isotope data was performed with the program Isoplot V.3.0 (5) using a <sup>187</sup>Re decay constant of 1.666 x 10<sup>-11</sup> year<sup>-1</sup> (6-8), 2σ uncertainties for <sup>187</sup>Re/<sup>188</sup>Os and <sup>187</sup>Os/<sup>188</sup>Os isotope ratios as determined by numerical error propagation, and the error correlation function (rho) (4).

Rhenium (11-39 ppb) and Os (467-1148 ppt) are strongly enriched in these shales relative to average present-day upper continental crust (~ 2 ppb Re and 30-50 ppt Os; 9-13). In addition, Re shows a pronounced enrichment in shales from the 145.22-148.32 m interval (22-39 ppb Re) relative to the 128.71-129.85 m interval (11-21 ppb). Isotope ratios for <sup>187</sup>Re/<sup>188</sup>Os and <sup>187</sup>Os/<sup>188</sup>Os range from 173 to 558 and from 7.4 to 74.0, respectively. Regression of the Re-Os

isotope data yields Model 1 dates of  $2495 \pm 18$  Ma ( $2\sigma$ ,  $n = 5$ ,  $\text{MSWD} = 0.95$ , initial  $^{187}\text{Os}/^{188}\text{Os} = 0.06 \pm 0.09$ ) and  $2464 \pm 41$  Ma ( $2\sigma$ ,  $n = 4$ ,  $\text{MSWD} = 0.48$ , initial  $^{187}\text{Os}/^{188}\text{Os} = 0.86 \pm 0.86$ ) for the 128.71-129.85 m and 145.22-148.32 m intervals, respectively. Combining the two data sets yields a Model 1 Re-Os date of  $2501.1 \pm 8.2$  Ma ( $\text{MSWD} = 1.1$ , initial  $^{187}\text{Os}/^{188}\text{Os} = 0.04 \pm 0.06$ ).

The initial  $^{187}\text{Os}/^{188}\text{Os}$  isotope composition derived from the regression records the Os isotope composition of the contemporaneous seawater at the time of sediment deposition (e.g., 14). Because the residence time of Os in present-day seawater is geologically short ( $\sim 10^4$ - $10^5$  years; 15, 16), it is usually necessary to restrict stratigraphic sampling intervals to  $\sim 1$  m or less to avoid initial Os isotope heterogeneity (e.g., 2-4, 7, 17). The sedimentation rate of the McRae Shale is not known, but during the span of geologic time covered by the  $\sim 20$  m of stratigraphy sampled here, the Os isotope composition of  $\sim 2.5$  Ga seawater probably changed. Accordingly, the Re-Os regression for the 128.71-129.85 m interval provides the most accurate and precise estimate of the  $^{187}\text{Os}/^{188}\text{Os}$  isotope composition of 2.5 Ga seawater ( $0.06 \pm 0.09$ ). This value overlaps the present-day Os isotope composition of chondrites and estimated values for the convecting and primitive upper mantle ( $\sim 0.13$ ; 18-20) and the Os isotope composition of chondrites at ca. 2.5 Ga ( $\sim 0.11$ ). These data indicate that the ocean Os budget was dominated by hydrothermal fluids and associated low- and high-T hydrothermal alteration of oceanic crust (21, 22), weathering of predominantly mafic rocks (23), and/or dissolution of cosmic dust.

### ***Total Organic Carbon Analyses***

Total organic carbon (TOC) was analyzed at the University of Washington using splits from the same powders analyzed for metals. In preparation for analyses, crushed rock powders were treated with HCl to remove any carbonate present. Specifically,  $\sim 10$  ml of 36.5 – 38.0 % HCl were added to  $\sim 0.3$ - $0.5$  g of sample and placed in a  $65^\circ\text{C}$  water bath overnight. The acidified samples were rinsed twice with Milli-Q water and dried in a  $65^\circ\text{C}$  oven. Samples were weighed before and after acidification to determine the fraction of carbonate. Tin capsules (5x9 mm) containing 0.1 – 0.2 mg of acidified sample were then prepared and analyzed via a Costech ECS 4010 Elemental Analyzer, coupled to a Thermo Scientific MAT 253. Samples were measured in triplicate to ensure reproducibility and those that did not meet a specific criterion ( $\text{range}_{\text{TOC}} \leq 0.5$  ‰;  $\text{standard deviation}_{\text{TOC}} \leq 0.4$  ‰) were re-analyzed until they did. An acetanilide reference material with known carbon content (71.09%) was analyzed at the beginning of each run and then after every two sets of triplicates. The TOC of the samples can be determined since the sum of the areas under the three  $\text{CO}_2$  peaks (masses 44, 45, and 46) as reported by the mass spectrometer is proportional to the weight of carbon in the sample being analyzed. Because the weight % C of the standard is known, a relationship between the sum of the areas and the weight of carbon needed to produce this sum can be determined. Applying the above relationship to the sum of the areas under the sample peaks gives the weight % C of the samples analyzed. Assuming that all carbonate carbon in the samples is lost during acidification, the calculated weight % C actually represents the weight % organic C of the acidified samples. The TOC values of the bulk samples are then determined by multiplying this value by the fraction of sample remaining after acidification.

**Table S1.** Average Mo data for Archean and Proterozoic pyritic black shales.

	Average Maximum Mo (ppm)	Average Minimum Mo (ppm)	Average Mo (ppm)	Average Mo/Al (ppm/wt%)	Average Mo/TOC (ppm/wt%)
Archean *	4	1	3	0.4	1.6
Proterozoic **	48	9	18	4	6
Phanerozoic**	270	60	160	27	28

\*Yamaguchi (24); \*\*Scott et al. (26)

Table S2. Geochemical data for McRae Shale samples.

depth (m)	Al wt %	Mn wt %	Fe wt %	Mo ppm	Re ppb	U ppm	Carbonate wt %	TOC wt %	S wt %	Mo/TOC ppm/wt%	Mo/Al ppm/wt%	Re/Al ppb/wt%	U/Al ppm/wt%	
ave upper crust*	8.04	0.06	3.5	1.50	1.00**	2.80					0.19	0.12	0.35	
											Enrichment Factor	Enrichment Factor	Enrichment Factor	
105.20	0.3	0.18	34.4	0.4	2.2	0.2					7.3	59.5	1.9	
107.25	0.8	0.14	35.5	0.6	1.2	0.4					3.6	11.7	1.4	
108.27	0.5	0.14	31.1	0.5	1.5	0.3					6.1	25.3	1.6	
108.54	0.3	0.11	28.4	0.2	0.3	0.1					3.1	7.4	0.5	
109.00	7.5	0.05	10.0	8.0	7.9	6.6	30.1	3.1	1.2	2.6	5.7	8.5	2.5	
110.70	5.9	0.08	2.5	8.7	12.1	5.3	24.6	3.5	0.5	2.5	7.8	16.3	2.6	
111.00	4.8	0.21	3.9	5.1	5.1	4.5	46.0	2.7	0.8	1.9	5.7	8.5	2.7	
112.52	5.6	0.18	3.0	6.8	5.5	4.9	38.8	3.7	0.5	1.9	6.5	7.8	2.5	
113.46	7.5	0.05	2.7	11.5	9.4	6.9	16.3	5.8	1.0	2.0	8.2	10.1	2.7	
114.50	2.5	0.42	2.3	2.2	2.5	2.2	71.6	2.2	0.7	1.0	4.8	8.0	2.5	
115.49	1.9	0.36	2.4	2.8	1.7	1.9	72.4	1.9	0.2	1.5	7.9	7.2	2.9	
116.49	4.2	0.25	2.4	7.8	5.7	4.0	55.3	3.6	0.5	2.2	10.1	11.0	2.7	
117.31	2.4	0.33	2.4	2.8	2.5	2.1	61.2	2.6	0.3	1.1	6.3	8.4	2.5	
118.13	3.2	0.29	2.3	4.3	5.7	2.7	57.6		0.6		7.2	14.4	2.5	
119.24	2.4	0.30	2.5	2.8	3.2	1.9	63.1	2.9	0.2	1.0	6.3	10.7	2.3	
120.42	1.6	0.31	2.7	1.7	1.5	1.3	68.6	1.9	0.2	0.9	5.8	7.7	2.4	
121.20	2.9	0.25	2.4	3.6	3.6	2.3	59.5	2.9	0.3	1.2	6.7	10.2	2.3	
121.39	2.9	0.30	2.5	3.7	5.2	2.5	68.8	2.4	0.4	1.5	6.8	14.4	2.5	
122.32	3.9	0.19	2.6	6.3	6.8	3.0	46.5	3.7	0.4	1.7	8.6	13.8	2.2	
123.22	2.9	0.25	3.0	2.8	2.9	2.2	61.3	2.3		1.2	5.2	8.2	2.2	
124.22	5.5	0.11	2.7	6.3	8.7	3.8	34.4	3.5	0.3	1.8	6.2	12.7	2.0	
125.25	3.6	0.20	8.1	11.5	41.1	3.1	49.7		5.4		17.1	91.7	2.5	
126.15	6.9	0.07	3.0	7.4	6.2	4.8	24.0	4.1	0.3	1.8	5.7	7.3	2.0	
127.25	7.4	0.07	3.2	10.4	11.3	5.3	18.0	6.9	0.9	1.5	7.6	12.4	2.1	
128.17	7.9	0.05	3.1	13.3	17.8	5.4	14.2	6.5	1.0	2.1	9.0	18.1	2.0	
129.01	8.1	0.04	3.1	9.2	12.0	5.4	12.1	6.1	1.2	1.5	6.1	12.0	1.9	
129.55	6.8	0.03	8.9	10.2	27.6	5.1	7.3	5.6		1.8	8.0	32.6	2.1	
130.06	7.8	0.04	2.5	13.0	26.2	5.4	9.5		0.7		8.9	27.0	2.0	
130.71	-pyl	5.7	0.07	7.3	7.3	9.7	13.0	5.5	5.4	1.3	6.8	13.7	1.9	
130.76	-pyl	6.3	0.07	2.4	6.0	10.7	12.0	6.2	0.4	1.0	5.1	13.6	1.9	
131.60	-pyl	8.0	0.02	7.8	13.8	17.3	5.4				9.2	17.4	1.9	
131.60	-pyl	6.3	0.02	16.4	10.9	11.5	3.6	5.9	3.9	2.8	9.2	14.6	1.7	
132.13	-pyl	6.8	0.04	2.5	14.7	18.4	5.2	8.6	6.8	0.5	11.6	21.9	2.2	
133.97	-pyl	7.8	0.08	4.2	19.4	26.8	4.5	11.1	7.7	0.6	2.5	13.3	1.7	
135.58	-pyl	4.2	0.21	13.7	8.3	12.5	3.3	14.3	7.2	14.3	1.2	10.7	2.3	
136.15	-pyl	6.5	0.04	4.4	15.2	21.3	5.3	4.2	8.2	3.9	1.8	12.5	2.3	
136.67	-pyl	6.8	0.06	6.1	17.3	18.8	7.7	6.2	7.7	5.3	2.3	13.6	3.3	
136.94	-pyl	5.3	0.05	9.3	17.5	20.6	4.4	13.6	9.0	8.7	1.9	17.5	31.0	2.4
137.31	-pyl	5.4	0.03	7.4	23.5	25.5	4.8	3.3		6.6		23.4	38.1	2.6
137.68	-pyl	4.6	0.04	9.8	11.9	15.5	3.6	5.7	9.4	10.5	1.3	13.9	27.0	2.2
137.96	-pyl	5.7	0.04	6.8	19.1	19.3	4.6	4.4	10.8	6.3	1.8	17.9	27.1	2.3
138.38	-pyl	6.0	0.03	6.8	19.0	27.0	4.3	6.7	10.9	6.0	1.8	16.9	36.1	2.0
138.74	-pyl	5.9	0.03	6.9	16.8	21.9	4.1					15.2	29.6	2.0
139.01	-pyl	5.0	0.03	11.9	19.0	29.6	3.4	4.7	11.0	11.6	1.7	20.3	47.6	2.0
139.65	-pyl	5.9	0.03	6.8	20.7	30.5	4.4	3.4	9.9		2.1	18.7	41.5	2.1
139.71	-pyl	5.1	0.01	23.9	9.9	12.8	2.2	2.4	5.5		1.8	10.4	20.2	1.3
139.97	-pyl	6.6	0.02	4.7	25.0	36.1	4.3	3.0	12.1	5.4	2.1	20.2	43.7	1.9
140.25	-pyl	6.0	0.02	6.1	22.6	38.4	3.4	3.3	12.4	6.9	1.8	20.1	51.1	1.6
140.50	-pyl	6.2	0.01	4.5	29.1	33.8	3.1	9.3	15.3	5.1	1.9	25.3	44.1	1.4
140.95	-pyl	6.0	0.02	5.3	30.5	41.5	3.7	4.1	16.1	6.3	1.9	27.3	55.6	1.8
141.17	-pyl	6.3	0.02	5.8	20.4	30.6	5.2	3.4	12.6	6.6	1.6	17.4	39.0	2.4
141.47	-pyl	6.4	0.02	5.2	21.9	31.6	3.2	7.4	13.0	5.3	1.7	18.3	39.6	1.4
141.72	-pyl	6.7	0.02	4.9	18.6	26.3	4.5		5.2			14.9	31.4	1.9
142.08	-pyl	6.5	0.01	4.3	19.1	26.7	4.1	3.9	11.6		1.6	15.7	33.0	1.8
142.60	-pyl	4.5	0.01	3.4	13.5	13.8	2.6			3.7		16.0	24.6	1.7
143.45	-pyl	3.7	0.05	7.9	41.4	37.1	2.5	9.6	13.1	7.7	3.2	59.4	79.9	1.9
144.36	-pyl	4.4	0.18	5.4	33.7	34.1	3.0	18.0	8.7	2.6	3.9	40.9	62.1	1.9
145.61	-pyl	6.1	0.04	5.1	40.1	36.3	4.8	13.5	13.4	2.0	3.0	35.3	47.9	2.3
146.45	-pyl	5.1	0.06	7.1	40.3	35.4	4.2	13.6	15.2	5.7	2.7	42.6	56.1	2.4
147.30	-pyl	5.8	0.04	4.5	27.1	25.5	6.3	10.1	12.6	2.3	2.2	25.0	35.3	3.1
148.27	-pyl	5.5	0.02	3.8	20.2	15.0	4.6	8.9	10.4	1.7	1.9	19.6	21.8	2.4
149.30	-pyl	7.1	0.02	4.3	37.1	37.9	5.2	9.8	12.1	3.7	3.1	27.9	42.9	2.1
150.24	-pyl	6.1	0.12	4.6	16.5	17.0	4.8	22.6	7.7	2.2	2.2	14.4	22.3	2.2
152.08	-pyl	5.7	0.03	2.7	7.3	10.0	4.1	17.8	5.7	1.5	1.3	6.9	14.2	2.1
152.65	-pyl	5.4	0.07	3.9	8.7	10.9	3.3	9.3	5.1	1.0	1.7	8.7	16.4	1.8
153.18	-pyl	6.4	0.02	2.7	6.7	6.6	3.4	9.1	4.0	0.6	1.7	5.7	8.3	1.5

S1

Table S1 con't. Geochemical data for McRae Shale samples.

	depth (m)	Al wt %	Mn wt %	Fe wt %	Mo ppm	Re ppb	U ppm	Carbonate wt %	TOC wt %	S wt %	Mo/TOC ppm/wt%	Mo/Al ppm/wt% 0.19	Re/Al ppb/wt% 0.12	U/Al ppm/wt% 0.35
	ave upper crust*	8.04	0.06	3.5	1.50	1.00**	2.80					Enrichment Factor	Enrichment Factor	Enrichment Factor
	154.43	7.1	0.02	6.8	6.7	8.2	4.5	15.0	4.1	2.5	1.6	5.1	9.3	1.8
	156.05	7.4	0.03	3.3	7.4	10.7	4.8	11.0	4.8	0.3	1.6	5.4	11.7	1.9
	157.80	7.2	0.08	8.0	8.0	10.2	4.7	24.3	4.3	2.4	1.9	6.0	11.5	1.9
	158.91	7.3	0.04	5.9	6.1	7.6	4.5	15.9	4.8	1.6	1.3	4.4	8.3	1.8
Siderite BIF	161.32	7.0	0.10	8.7	4.9	10.8	4.9	22.6	5.8	1.6	0.8	3.7	12.4	2.0
	162.80	5.4	0.21	18.9	4.0	4.7	3.3	51.0	3.3		1.2	4.0	7.1	1.7
	163.95	5.6	0.18	20.1	5.1	6.5	3.0	52.4	3.2	2.2	1.6	4.8	9.3	1.5
	165.56	3.6	0.29	18.1	3.3	5.5	2.2	52.1	2.9	0.8	1.2	4.9	12.4	1.8
	167.76	2.6	0.37	15.0	1.4	2.4	1.8	44.4	1.8	0.5	0.8	3.0	7.3	2.0
	168.36	3.1	0.40	16.0	3.3	3.2	2.0	45.4	1.9	0.9	1.8	5.7	8.1	1.8
	168.90	2.2	0.49	19.7	1.2	2.1	1.3	52.1	1.9	2.4	0.6	3.0	7.9	1.7
	169.28	4.5	0.30	13.5	2.0	4.7	3.8	32.9	2.7	1.5	0.8	2.5	8.4	2.5
	169.47	2.8	0.29	19.8	2.4	3.3	1.8	43.6	2.0	9.1	1.2	4.6	9.4	1.8
	169.68	3.5	0.27	12.8	1.8	2.6	1.8	50.7	2.0	1.5	0.9	2.8	6.0	1.5
	169.94	1.6	0.54	21.2	1.4	1.6	1.0	39.3	2.5	3.5	0.6	4.6	8.0	1.8
	170.17	3.8	0.37	15.7	2.1	3.2	2.9	50.5	2.1	2.4	1.0	2.9	6.7	2.2
	170.39	2.8	0.48	18.5	1.6	2.8	1.7	48.8	2.4	3.1	0.7	3.0	8.0	1.8
	170.55	3.6	0.39	16.2	2.2	4.3	2.6	27.2	3.1	2.6	0.7	3.3	9.6	2.0
170.86	4.4	0.33	13.7	1.9	3.8	3.6	41.1	2.2	1.8	0.9	2.3	7.0	2.4	
170.94	3.5	0.35	16.6	2.0	3.5	2.2	28.0	3.0	5.4	0.7	3.1	8.0	1.8	
171.22	4.4	0.27	13.8	2.9	4.1	3.4	26.6	2.8	3.2	1.0	3.5	7.4	2.2	
S2	173.09	5.5	0.16	13.0	3.4	4.0	3.3	31.5	3.1	1.7	1.1	3.3	5.8	1.7
	173.50	5.6	0.26	13.9	3.0	4.8	3.7	36.4	2.7	4.4	1.1	2.9	6.9	1.9
	173.73	4.0	0.42	16.8	2.5	4.5	2.0	42.0	2.8	2.2	0.9	3.3	9.1	1.5
	174.67	1.9	0.14	4.8	0.9	1.3	1.0	33.0	2.9	3.2	0.3	2.6	5.3	1.5
	175.51	5.9	0.20	9.2	3.3	6.1	4.3	23.8	3.8	2.4	0.9	3.0	8.3	2.1
	177.10	6.5	0.16	8.8	3.1	8.7	4.6	20.0	5.0	3.0	0.6	2.6	10.8	2.1
	178.61	6.3	0.16	7.3	3.2	7.4	3.7	15.2	4.9	3.5	0.7	2.7	9.4	1.7
	178.83	6.2	0.12	5.2	3.4	10.1	3.1	16.6	6.3		0.5	2.9	13.0	1.4
	179.05	6.2	0.17	7.6	3.0	7.9	3.9	15.9	4.7	3.1	0.6	2.6	10.2	1.8
	180.33	5.2	0.25	9.3	2.9	7.9	2.8	19.9	5.0	3.4	0.6	3.1	12.3	1.6
	181.20	4.8	0.32	10.1	2.0	9.3	3.0	23.8	4.2	2.7	0.5	2.3	15.8	1.8
	182.50	5.4	0.09	5.1	2.5	4.3	3.0	14.1	4.4	1.4	0.6	2.5	6.4	1.6
	183.65	4.8	0.44	8.0	2.4	4.1	2.9	22.2	3.1	2.1	0.8	2.7	7.0	1.8
	185.43	3.4	0.56	10.2	1.8	2.9	2.2	34.1	2.5	1.2	0.7	2.8	6.8	1.8
	187.46	6.0	0.10	5.7	3.2	5.0	4.2	13.7	3.6	1.5	0.9	2.9	6.8	2.0
	188.01	5.5	0.18	6.7	4.6	8.2	3.6	17.1	4.0	3.0	1.2	4.5	12.1	1.9
	188.87	4.9	0.19	7.0	7.7	5.3	3.5	22.7	3.3	1.5	2.3	8.5	8.8	2.0
189.39	4.8	0.30	6.7	3.6	11.8	3.9					4.0	19.6	2.3	

\* Average upper crust data from Taylor and McLennan (1985); \*\*average [Re] from Selby et al., (2007).

**Table S3.** Re-Os data for Mt. McRae Shale samples.

Re-Os abundance and isotope data for the Mt. McRae Shale, western Australia

Sample	Re (ppb)	Os (ppt)	<sup>192</sup> Os (ppt)	<sup>187</sup> Re/ <sup>188</sup> Os	<sup>187</sup> Os/ <sup>188</sup> Os	rho
ABDP9-128.71	11.59	628.8	133.2	173.11 (1.42)	7.3989 (0.0675)	0.717
ABDP9-128.84	11.49	513.8	86.1	265.57 (3.12)	11.3592 (0.1463)	0.822
ABDP9-129.15	13.32	467.3	47.4	558.35 (10.44)	23.6301 (0.4745)	0.895
ABDP9-129.36	20.94	792.7	96.8	430.21 (4.44)	18.3693 (0.1997)	0.830
ABDP9-129.85	21.04	761.0	83.4	501.84 (5.43)	21.3396 (0.2533)	0.808
ABDP9-145.22	39.06	1148.2	44.6	1742.85 (23.25)	73.9781 (1.0922)	0.836
ABDP9-146.08	27.20	820.3	39.2	1381.41 (19.89)	58.7478 (0.8446)	0.937
ABDP9-147.10	28.60	911.3	58.8	967.45 (10.94)	41.5033 (0.5201)	0.809
ABDP9-148.32	21.94	681.0	39.2	1113.77 (16.10)	47.4586 (0.6796)	0.945

Note: Numbers in parentheses denote measured 2 $\sigma$  uncertainty in the <sup>187</sup>Re/<sup>188</sup>Os and <sup>187</sup>Os/<sup>188</sup>Os isotope ratios as determined by numerical error propagation.

Total procedural blanks for Re and Os were 9.5  $\pm$  0.3 pg and 0.39  $\pm$  0.25 pg, respectively.

<sup>187</sup>Os/<sup>188</sup>Os of 0.224  $\pm$  0.068 (1 $\sigma$ , n=4).



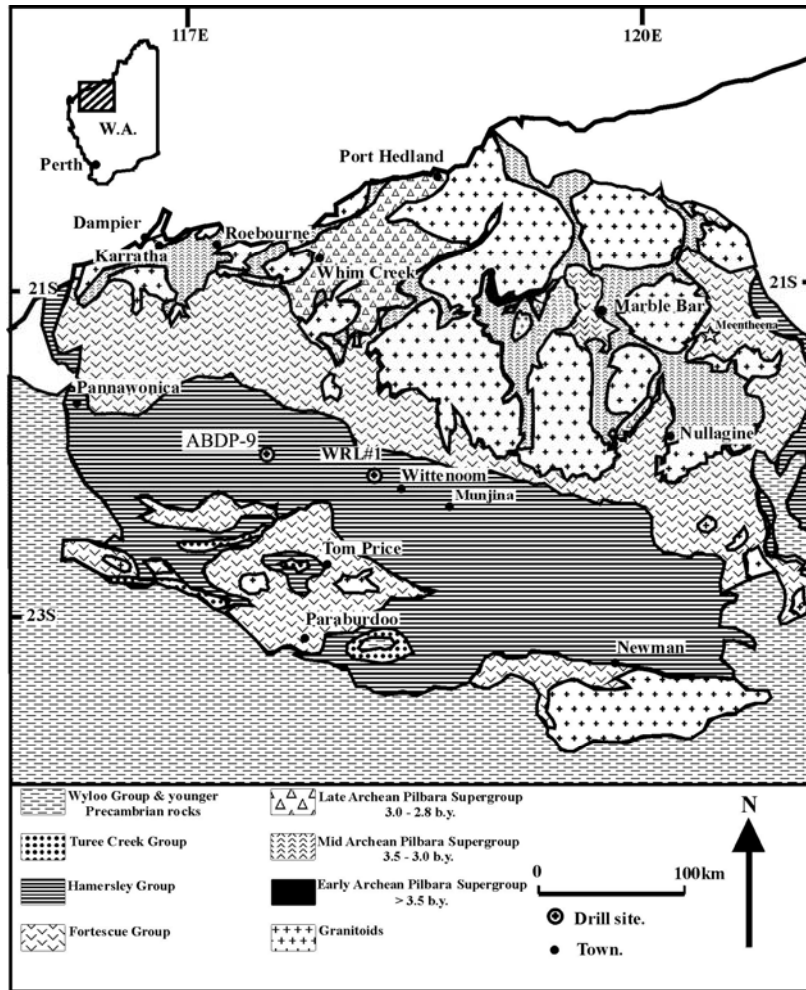


**Figure S1.** Simplified geologic map of the Pilbara Craton showing location of the ABDP-9 drill site.

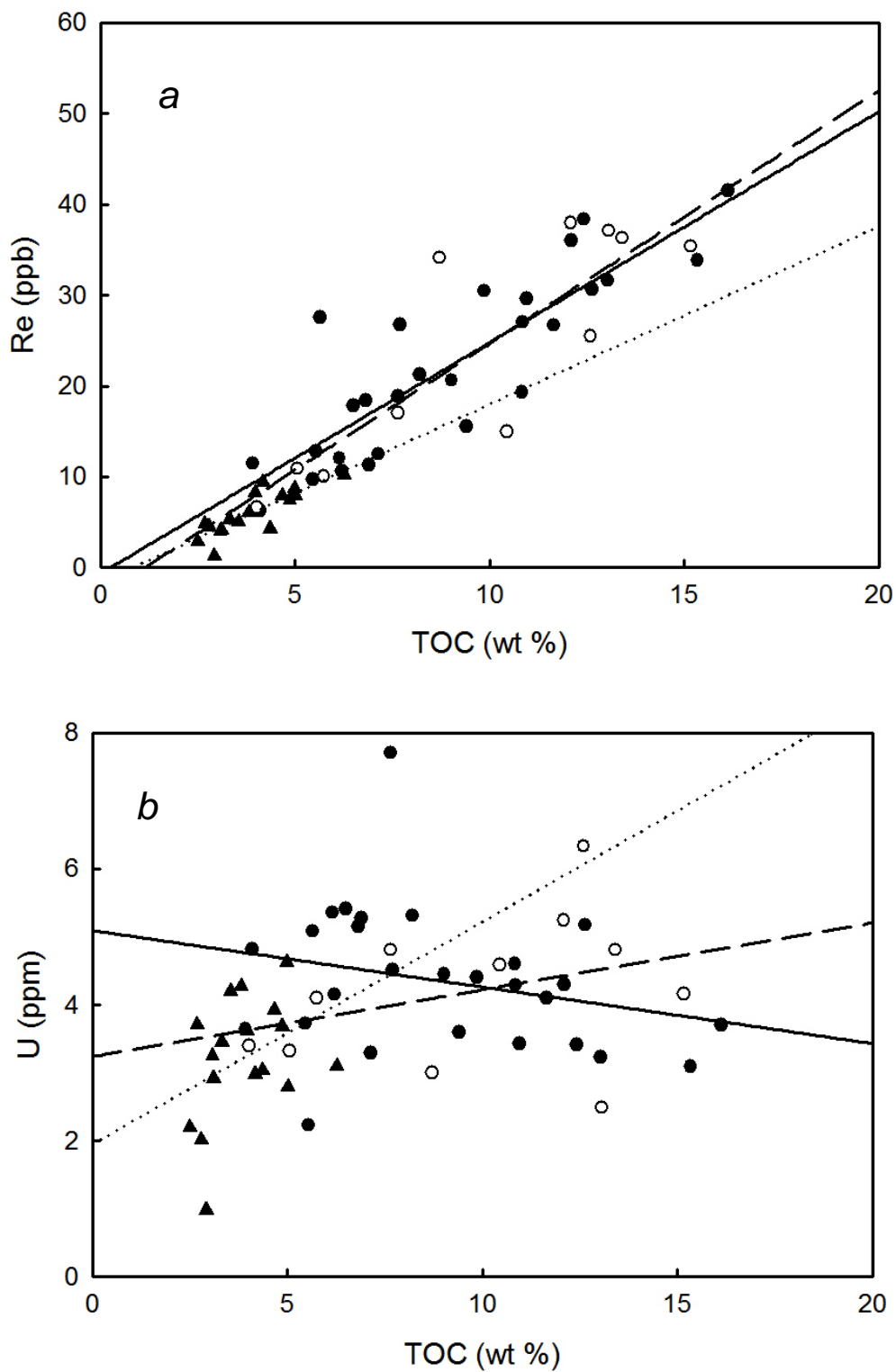


**Figure S2.** Relationship between (a) Re and TOC and (b) U and TOC in organic carbon-rich, pyritic intervals in the Mt. McRae Shale. Circles are from interval S1 (125.5 – 153.3 m). The metal-enriched zone of S1 below 143 m (open circles) is differentiated from the upper zone, (solid circles). Triangles are from interval S2 (173.0 – 189.7 m).

## References

1. H. Ohmoto, Y. Watanabe, H. Ikemi, S. R. Poulson, B. E. Taylor, *Nature* **442**, 908 (2006).
2. R. A. Creaser, P. Sannigrahi, T. Chacko, D. Selby, *Geochim. Cosmochim. Acta* **66**, 3441 (2002).
3. D. Selby, R. A. Creaser, *Chem. Geol.* **200**, 225 (2003).
4. B. S. Kendall, R. A. Creaser, G. M. Ross, D. Selby, *Earth Planet. Sci. Lett.* **222**, 729 (2004).
5. K. Ludwig, *User's manual for Isoplot/Ex rev. 3.00: A Geochronological Toolkit for Microsoft Excel*, Special Publication 4 (Berkeley Geochronology Center, Berkeley, 2003), pp. 70.
6. M. I. Smoliar, R. J. Walker, J. W. Morgan, *Science* **271**, 1099 (1996).
7. D. Selby, R. A. Creaser, *Geology* **33**, 545 (2005).
8. D. Selby, R. A. Creaser, M. G. Fowler, *Geochim. Cosmochim. Acta* **71**, 378 (2007).
9. B. K. Esser, K. K. Turekian, *Geochim. Cosmochim. Acta* **57**, 3093 (1993).
10. B. Peucker-Ehrenbrink, B. M. Jahn, *Geochem. Geophys. Geosys.* **2** (2001).
11. Y. Hattori, K. Suzuki, M. Honda, H. Shimizu, *Geochim. Cosmochim. Acta* **67**, 1195 (2003).
12. W. D. Sun, V. C. Bennett, S. M. Eggins, V. S. Kamenetsky, R. J. Arculus, *Nature* **422**, 294 (2003).
13. B. Peucker-Ehrenbrink, *Geochim. Cosmochim. Acta* **60**, 3187 (1996).
14. G. Ravizza, K. K. Turekian, *Earth Planet. Sci. Lett.* **110**, 1 (1992).
15. R. Oxburgh, *Earth Planet. Sci. Lett.* **159**, 183 (1998).
16. S. Levasseur, J. L. Birck, C. J. Allegre, *Earth Planet. Sci. Lett.* **174**, 7 (1999).
17. B. S. Kendall, R. A. Creaser, paper presented at the Sixteenth Annual V. M. Goldschmidt Conference, Melbourne, Australia, 27 Aug to 1 Sep 2006.
18. T. Meisel, R. J. Walker, A. J. Irving, J. P. Lorand, *Geochim. Cosmochim. Acta* **65**, 1311 (2001).
19. R. J. Walker *et al.*, *Geochim. Cosmochim. Acta* **66**, 4187 (2002).
20. R. J. Walker, H. M. Prichard, A. Ishiwatari, M. Pimentel, *Geochim. Cosmochim. Acta* **66**, 329 (2002).
21. M. Sharma, G. J. Wasserburg, A. W. Hofmann, D. A. Butterfield, *Earth Planet. Sci. Lett.* **179**, 139 (2000).
22. R. R. Cave, G. E. Ravizza, C. R. German, J. Thomson, R. W. Nesbitt, *Earth Planet. Sci. Lett.* **210**, 65 (2003).
23. C. E. Martin, B. Peucker-Ehrenbrink, G. J. Brunskill, R. Szymczak, *Earth Planet. Sci. Lett.* **183**, 261 (2000).
24. K. Yamaguchi, thesis, Pennsylvania State University (2002).
25. C. Scott, paper presented at the 2006 Annual Meeting of the Geologic Society of America, 22 October 2006.